

Biodiesel production from jatropha seeds with bead-type heterogeneous catalyst

Jaegyoo Woo*, Rajendra Joshi**, Young-Kwon Park***, and Jong-Ki Jeon*[†]

*Department of Chemical Engineering, Kongju National University, Cheonan 31080, Korea

**Department of Chemical Science and Engineering, School of Engineering, Kathmandu University, Dhulikhel, Nepal

***School of Environmental Engineering, University of Seoul, Seoul 02504, Korea

(Received 6 January 2021 • Revised 29 January 2021 • Accepted 1 February 2021)

Abstract—This study adapted two types of heterogeneous catalysts to the process of manufacturing biodiesel through a two-stage process using Jatropha oil as a raw material. The acid value of Jatropha oil prepared in this study was 11.3 mgKOH/g, and it could be reduced to less than 0.4 mgKOH/g via 2 h of esterification using the Amberlyst-15 catalyst. The pretreated oil was used as a raw material for transesterification in a Carberry spinning catalyst basket reactor equipped with a bead-type dolomite catalyst, as the bead-type dolomite catalyst prepared with 20 wt% pseudoboehmite sol as an inorganic binder was found to be the optimal catalyst for the transesterification reaction. The spent dolomite bead catalyst could be regenerated and reused twice without a loss of activity during transesterification. However, the catalyst when repeatedly regenerated three times nearly lost its active sites, which is attributed to the conversion of CaO to CaCO₃ during the regeneration and reuse procedure.

Keywords: Jatropha Oil, Transesterification, Dolomite, Bead-type Catalyst, Regeneration

INTRODUCTION

With the development of industry, energy consumption has increased, resulting in rising oil prices and greenhouse gas emissions. Accordingly, the Renewable Fuel Standard system, mainly related to transportation fuel and involving the mixing of a certain amount of biodiesel with petroleum diesel, is being introduced worldwide. Biodiesel can be manufactured from plant oils and animal fats. The first generation of biodiesel uses cooking oil and food crops as raw materials, with canola oil, palm oil, and sunflower oil commonly used [1,2]. The second generation of biodiesel uses non-edible crops as raw materials, typically Jatropha oil, Kapok oil, Rubber tree oil, and Jojoba oil [3-5]. Among them, studies of biodiesel synthesis using oil extracted from Jatropha plants, which have easy cultivation conditions even in harsh environments, are being actively conducted [6,7].

Biodiesel consists of fatty acid methyl ester (FAME) and is synthesized by the transesterification of 1 M of triglyceride and 3 M of methanol [8]. In general, it proceeds as a catalytic reaction at a temperature of 60-100 °C and atmospheric pressure. As a catalyst used in the transesterification reaction, a homogeneous alkali catalyst such as NaOH or KOH is used [9]. However, separating the homogeneous catalyst from the biodiesel produced is complex, making it very difficult to reuse the catalyst. Moreover, a wastewater treatment process is inevitable after the separation process. To solve the problems associated with the homogeneous catalyst process, research to facilitate catalyst reuse using heterogeneous catalysts (solid catalysts) instead of homogeneous catalysts is actively underway [10]. It has been reported that CaO, MgO, and hydrotalcite, among

other materials, are currently being studied as heterogeneous basic catalysts for transesterification [3,11-17].

On the other hand, the raw material of the second generation of biodiesel contains a high content of free fatty acid (FFA) in addition to triglyceride. When the FFA content in the raw material exceeds 2.5 wt%, it is very difficult to apply a conventional basic catalyst because soap is easily produced by the interaction between the fatty acid and the basic catalyst [18]. To avoid soap formation, the FFA must be removed from the system or converted into a more valuable product. Typically, physical purification is more suitable to remove FFA. However, the conversion of FFA to biodiesel through the esterification reaction can increase the productivity of the biodiesel manufacturing process. Owing to this advantage, a two-stage process in which an esterification reaction is conducted using a solid acid catalyst in stage 1 with a subsequent transesterification process using a solid base catalyst in stage 2 is drawing attention [15].

This study adapted two types of heterogeneous catalysts to the process of manufacturing biodiesel through a two-stage process using Jatropha oil as a raw material. In the first stage, Amberlyst-15 was applied as a solid acid catalyst for the esterification reaction of the FFA contained in Jatropha oil, and optimal conditions for reducing the content of FFA were selected. In the second step, dolomite, an inexpensive basic catalyst, was applied to the transesterification reaction [14,15]. An organic binder and an inorganic binder were added to the dolomite powder to establish a shaping method for manufacturing in a bead form. The effects of the physicochemical properties of the catalyst on the catalytic performance were studied. Transesterification reactions using the bead-type dolomite catalyst were performed in a catalyst basket reactor. To the best of our knowledge, a bead-type dolomite catalyst in a catalyst basket reactor is utilized for the first time here during the transesterification of Jatropha oil. This study also focused on a regenera-

[†]To whom correspondence should be addressed.

E-mail: jkjeon@kongju.ac.kr

Copyright by The Korean Institute of Chemical Engineers.

tion method for the spent bead-type dolomite catalyst and its reuse during the transesterification of Jatropha oil.

EXPERIMENTAL

1. Preparation of Jatropha Oil and Determination of the FFA Content

A custom-made oil press was used to press and extract oil from Jatropha seeds. The kernels of the Jatropha seeds were separated manually. The white and soft part of the seed was put into the oil press. The temperature on the screw was around 80 °C. The oil was collected by filtering out the seed cake with the help of a sieve. The total weight of the seeds and the kernels was 3 kg and 1.5 kg, respectively. After the pressing process, an amount of 750 mL of Jatropha oil was obtained.

The FFA content in the Jatropha oil was determined by a chemical titration method (ASTM D 6751). Here, 2.5 grams of Jatropha oil and 50 ml of a mixture of toluene (99.5%, Sigma Aldrich) and ethanol (95.0%, Sigma Aldrich) at a 1 : 1 volume ratio were measured and placed into a flask. Approximately 50 ml of ethanol (95.0%, Sigma Aldrich), which was previously neutralized by adding 2 ml of phenolphthalein (Sigma Aldrich), was then added to the oil in the flask. The mixture was then titrated with a KOH solution (0.01 N) and the end point value of the titration was recorded. The acid value was calculated by Eq. (1) and the FFA content could subsequently be determined as half of the acid value.

Acid value (mgKOH/g)

$$= \left[\frac{56.11 \times \text{Consumption of KOH Solution} \times \text{Concentration of KOH Solution}}{\text{Sample (g)}} \right] \quad (1)$$

2. Catalyst Preparation

Amberlyst-15 (hydrogen form) in a bead form (diameter, 0.5 mm) was purchased from Sigma Aldrich. Dolomite powder ($\text{CaMg}(\text{CO}_3)_2$) was purchased from Sungshin Co. Ltd. and shaped into beads through the following procedures. The dolomite powder was fired at 800 °C for two hours. To shape the dolomite powder into the bead form, methyl cellulose (Mecellose, Lotte Fine Chemical) and pseudoboehmite sol were used as organic and inorganic binders, respectively. 27.8 g of pseudoboehmite powder (Capatal B, Sasol) was mixed with 56.8 g of distilled water and stirred at 300 rpm for 30 min. A solution of 1.2 g of nitric acid (60%, Aldrich) and 14.2 g of distilled water was added and stirred for 40 h to prepare pseudoboehmite sol. Dolomite powder 100 g, methyl cellulose 5 g, and a certain amount of pseudoboehmite sol were mixed. An appropriate amount of distilled water was added to the mixture and sufficiently kneaded using a kneader. The dough was then shaped into beads using a custom-made molding machine. Subsequently, the shaped dolomite beads were dried at 100 °C and then calcined at 550 °C to complete the creation of the dolomite bead catalyst with a diameter of 2 mm. The completed dolomite bead catalyst is referred to here as Dolomite-bead-PB-10, where the number indicates the weight of the pseudoboehmite sol added based on 100 g of dolomite powder.

3. Characterization of the Dolomite Bead Catalyst

To measure the specific surface area and pore size of the catalyst, a nitrogen adsorption experiment was performed using a Bel-sorp II device from BEL Japan. After impurities on the catalyst surface were removed under a vacuum at 200 °C, the adsorption-desorption isotherm was obtained using nitrogen at -196 °C. The specific surface area and the pore size of the mesopore were calculated using the Brunauer Emmett Teller (BET) method and the Barret Joyner Halenda (BJH) method, respectively. The micropore volume was measured by the t-plot method.

A carbon dioxide temperature-desorption experiment (CO_2 -TPD) was used to analyze the basicity of the catalyst sample. This was done with a BELCAT-B device (MicrotracBEL Corp.). In this experiment, 0.5 g of the catalyst sample in a quartz tube was pretreated under a helium gas flow (50 ml/min) at 500 °C. The cell remained at 500 °C for 60 min before it was cooled to 50 °C. The samples were saturated for 30 minutes in a gas mixture flow of 3% CO_2 /He at 50 °C. The total flow rate was 50 ml/min. Then, the catalyst samples were cleaned in a He flow until a constant baseline level was reached. CO_2 -TPD measurements were taken in the temperature range of 50-800 °C at a rate of 10 °C/min under He (50 ml/min) flow. The evolved carbon dioxide was detected by a thermal-conductivity detector, calibrated by the peak area of known pulses of CO_2 . The crystalline structure of the powder samples was analyzed by a Rigaku MiniFlex 600 device operating with a $\text{Cu K}\alpha$ radiation. XRD data were collected with a scan speed of 10°/min in a 2θ range of 5-90 degrees.

4. Esterification of Jatropha Oil over Amberlyst-15

To reduce the acid value of the Jatropha oil, the esterification reaction was carried out in a batch reactor. During this reaction, 70 g of Jatropha oil and 10.5 g of Amberlyst-15 were placed in a reactor and heated with a heating mantle. When the temperature in the reactor reached 60 °C, 21 g of methanol (99.5%, Sigma Aldrich) was added into the reactor and stirred at a speed of 150 rpm for 4 h. The product was collected at 1 h intervals, after which the FFA content of the product was determined by the chemical titration method described in section 2.1.

5. Transesterification of Jatropha Oil over Dolomite Bead Catalysts

The transesterification reaction involved using oil with a reduced free fatty acid content as a raw material. For the transesterification reaction, a Carberry spinning catalyst basket reactor (volume 250 ml) equipped with a flat blade basket was used [19]. Fig. 1 shows a picture of the bead-type catalysts mounted in a Carberry spinning catalyst basket reactor. In this case, 130 g of the pretreated Jatropha oil and 13 g of catalyst were added to the reactor and the reactor was heated using a heating block. When the temperature of the reactor reached 65 °C, 50 g of methanol was added to the reactor and stirred at 150 rpm. The product was collected at 1 h intervals and then analyzed by a gas chromatograph (YL6500 GC, Young In Chromass) equipped with a capillary column (HP-Innowax, 30 m×0.530 mm×1 μm) and a flame ionization detector. The internal standard used for 0.1 g of the sample was a solution of 4 mg of methyl heptadecanoate (99%, Sigma-Aldrich) in 1 mL of n-heptane (99%, Baker). The FAME content was calculated by Eq. (2).

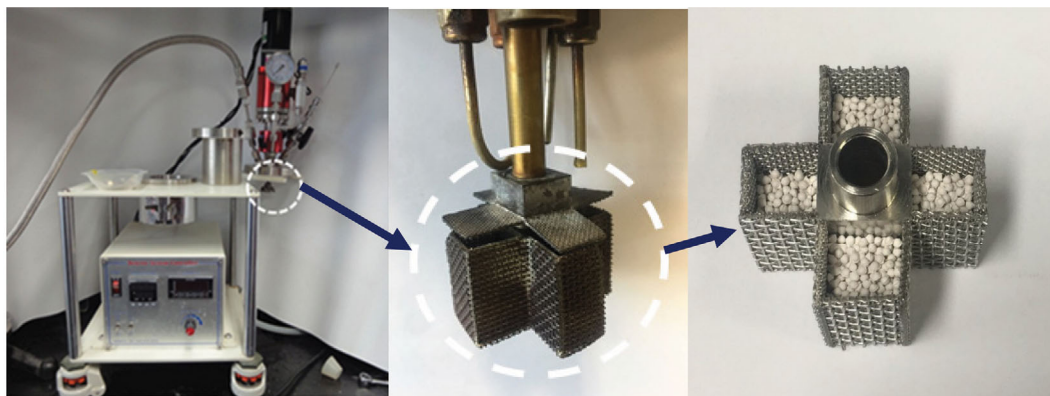


Fig. 1. Image of the bead-type catalysts mounted on a Carberry spinning catalyst basket reactor.

FAME conversion(%)

$$= \frac{\text{Total peak area of methyl ester} - \text{Peak area of internal standard}}{\text{Peak area of internal standard}} \times \frac{\text{Concentration of internal standard}}{\text{Sample (g)}} \quad (2)$$

6. Catalyst Regeneration and Reuse in the Transesterification of Jatropha Oil

After the transesterification reaction was completed, all of the products were recovered and the spent catalyst was washed as it was installed in the catalyst basket. Methanol was added to the reactor and stirred at 150 rpm for 2 h at room temperature. After

the washing step, the recovered catalyst was dried in an oven at 100 °C for 3 h in an air atmosphere. After drying, the regenerated catalyst was adapted again for the transesterification reaction.

RESULTS AND DISCUSSION

1. Catalysts Characterization

The N₂ adsorption isotherm of the dolomite powder (Fig. 2) shows that it corresponds to Type III in the IUPAC classification, indicating that the adsorbed nitrogen molecules are gathered around the most favorable sites on the surface of a non-porous or macroporous solid, while micropores are mostly undeveloped [20,21]. As indicated in Fig. 1, the dolomite bead samples exhibited a Type V isotherm in the IUPAC classification. Given the similarity to Type III in the low P/P₀ range, this can be attributed to the presence of a non-porous solid. At a higher P/P₀ ratio, the isotherms showed a Type H3 hysteresis loop in de Boer's classification, as determined by non-rigid aggregates of plate-like particles, but also if the pore network consists of macropores which are not completely filled with pore condensate [20].

The structural parameters as determined from the N₂ isotherms are listed in Table 1, including the total BET surface area (S_{BET}), single-point adsorption total pore volume measured at P/P₀=0.99 (V_p), the average pore diameter (D_p) as calculated by BJH desorption, and the t -plot micropore volume (V_{micro}). The BET surface area and pore volume of the bead-type dolomite catalysts are much higher than those of dolomite powder, which means that the surface area and pore volume are considerably enhanced through the foaming procedure in comparison with the powder-type catalyst. This is attributed to the mesopores and macropores generated by the decomposition of the organic binder in the bead-type catalysts during calcination, which can be confirmed through the pore size distribution of the catalyst samples in Fig. 3. Meanwhile, the micropore volume was analyzed using the t -plot method, but the micropore volume was mostly negligible in all of the dolomite catalyst samples. From the N₂ adsorption results, it was observed that mesopores and macropores were well generated during the formation of the bead-type dolomite, whereas micropores remained undeveloped.

The BET surface area of the bead-type dolomite catalysts was in

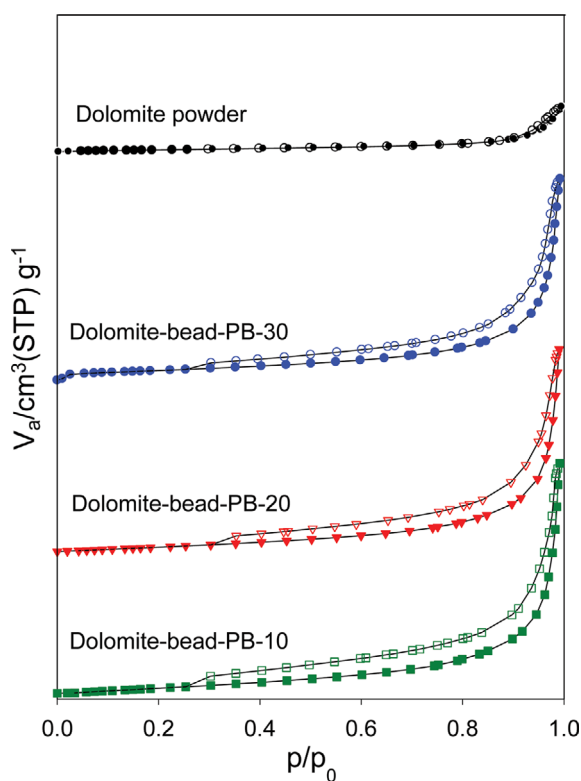


Fig. 2. N₂ adsorption isotherms of various catalysts (filled symbol: adsorption, empty symbol: desorption).

Table 1. Textural properties of the dolomite powder, bead-type catalysts and regenerated catalysts

Catalyst	S_{BET}^a (m^2/g)	D_p^b (nm)	V_p^c (cm^3/g)	V_{micro}^d (cm^3/g)
Dolomite powder	22	21	0.09	ND ^e
Dolomite-bead-PB-10	67	90	0.48	ND
Dolomite-bead-PB-20	57	58	0.43	ND
Dolomite-bead-PB-30	52	58	0.42	ND
Dolomite-bead-PB-20, 1st regeneration	57	78	0.32	ND
Dolomite-bead-PB-20, 2nd regeneration	33	67	0.27	ND
Dolomite-bead-PB-20, 3rd regeneration	30	51	0.39	ND

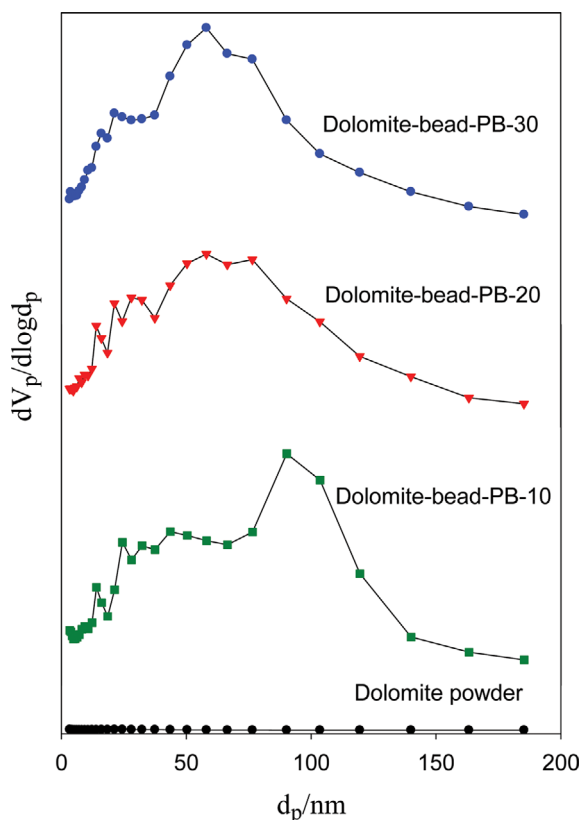
^aMeasured in the range of $P/P_0=0.05-0.30$

^bDetermined at $P/P_0=0.99$

^cAverage pore sizes calculated by BJH method from the adsorption branches

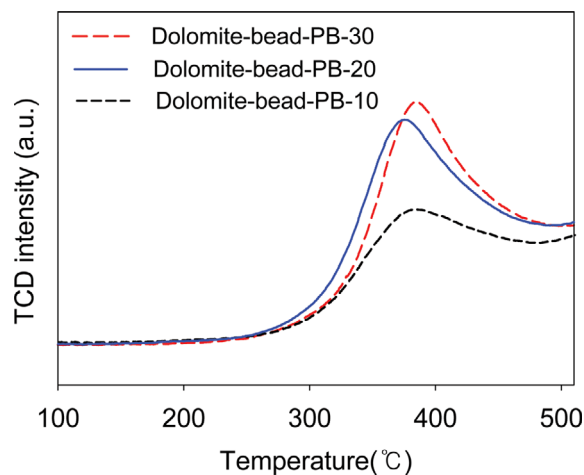
^dMicropore volume measured by the t -plot method

^eNot detected.

**Fig. 3. Pore size distribution of various catalysts.**

the range of 52–67 m^2/g . The order of the surface area and pore volume is as follows: Dolomite-bead-PB-10>Dolomite-bead-PB-20>Dolomite-bead-PB-30, which indicates that the surface area and pore volume decreased as the content of the inorganic binder increased.

The strength and number of basic sites are reflected in the desorption temperature and peak area of the CO_2 -TPD profile, respectively [22,23]. The basic sites of the bead-type dolomite samples were characterized by the CO_2 -TPD, and these profiles are compared in Fig. 4. The CO_2 -TPD spectra of the bead-type dolomite samples showed single desorption peak in the range of 370–380 °C.

**Fig. 4. CO_2 -TPD of bead-type dolomite catalysts.**

The peak temperatures of the CO_2 -TPD profiles of the three catalysts were nearly identical, which indicates that there is no significant difference in the strength of the basic sites of the three catalysts. Also, the amounts of CO_2 desorbed from the Dolomite-bead-PB-20 and Dolomite-bead-PB-30 catalysts were greater than that desorbed from the Dolomite-bead-PB-10 catalyst. This indicates that the number of basic sites on the Dolomite-bead-PB-20 and Dolomite-bead-PB-30 catalysts was higher than the number on the Dolomite-bead-PB-10 catalyst.

2. Esterification over the Amberlyst-15 Catalyst for the FFA Reduction of Jatropha Oil

The maximum FFA content in bio-oil acceptable in an alkali-catalyzed system is below 2.5 wt% [24,25]. If the FFA content of the oil exceeds 2.5 wt%, i.e., if the acid value exceeds 5.0 mgKOH/g, esterification is required before the transesterification process. The acid value of the Jatropha oil prepared in this study was 11.3 mgKOH/g and esterification was performed using the Amberlyst-15 catalyst to lower it to less than 5.0 mgKOH/g. The first purpose of this study was to explore the optimal conditions for the esterification of FFA in Jatropha oil and methanol using the Amberlyst-15 catalyst.

Initially, we examined the effect of the agitation speed when

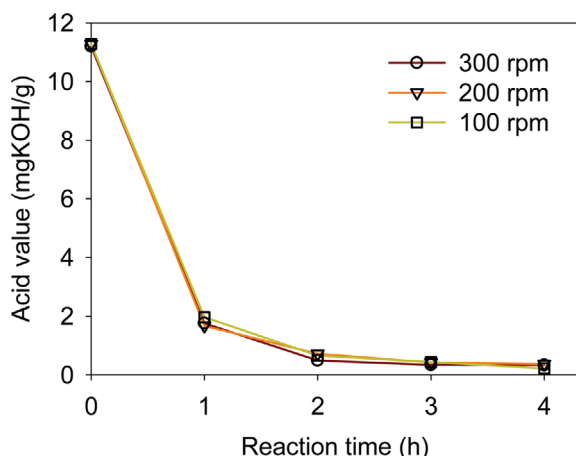


Fig. 5. Effects of the stirring speed on the esterification of Jatropha oil using the Amberlyst-15 catalyst (reaction condition: methanol/oil mole ratio=10, amount of catalyst based on oil=15 wt%, reaction temperature of 65 °C).

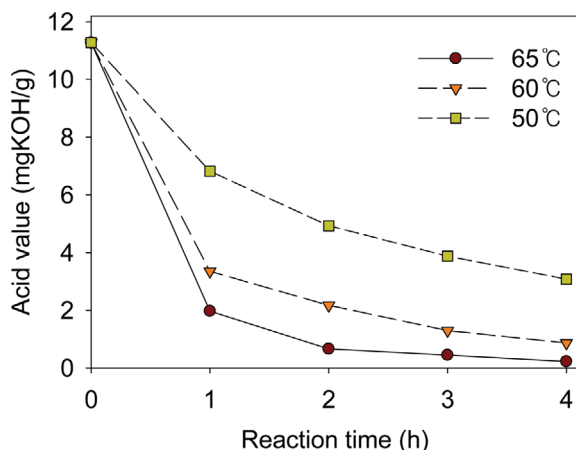


Fig. 6. Effects of the reaction temperature on the esterification of Jatropha oil using the Amberlyst-15 catalyst (reaction condition: methanol/oil mole ratio=10, amount of catalyst based on oil=15 wt%, stirring speed=100 rpm).

increasing it to 300 rpm on the esterification of FFA and methanol at a reaction temperature of 65 °C. As shown in Fig. 5, increasing the stirring speed to 300 rpm does not affect the esterification. Based on the phenomenon by which the catalytic activity did not increase with an increase in the stirring speed in a batch reactor, it can be assumed that the reactants and products are affected by the internal diffusion limitation in the bead-type catalyst pores rather than by any external diffusion limitation [26,27]. Therefore, 100 rpm was considered sufficient as the stirring speed to promote the esterification reaction. Through this experiment, it was observed that the acid value rapidly decreases to less than 2.0 mgKOH/g after 1 h of reaction using 15 wt% of the Amberlyst-15 catalyst; it can eventually be reduced to less than 0.4 mgKOH/g after 2 h of the reaction. Furthermore, because the decrease in the acid value scarcely progressed after the reaction time of 120 min, 120 min was determined as the optimal reaction time.

The effects of the reaction temperature on the esterification reac-

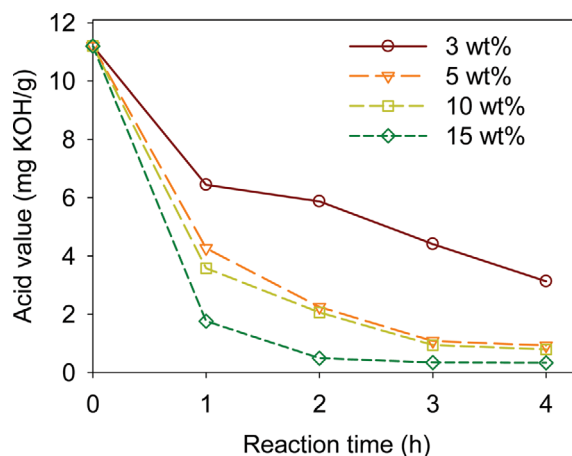


Fig. 7. Effects of the catalyst content on the esterification of Jatropha oil using the Amberlyst-15 catalyst (reaction condition: methanol/oil mole ratio=10, reaction temperature of 65 °C, stirring speed=100 rpm).

tion are shown in Fig. 6. As the reaction temperature increased from 50 °C to 65 °C, the rate of FFA removal was noticeably faster and the acid value decreased to 0.4 mgKOH/g after 2 h at 65 °C and to 0.22 mgKOH/g after 4 h. Fig. 7 shows the effect of the amount of catalyst used on the FFA removal rate. It was found that the acid value decreased rapidly as the amount of catalyst used was increased to 15 wt%. If the amount of catalyst used becomes too large, the operation of the reactor is restricted; accordingly, a catalyst amount of 15 wt% relative to the amount of oil was selected as the optimal catalyst amount. Consequently, the optimal reaction conditions for reducing FFA using the Amberlyst-15 catalyst were found to be a stirring speed of 100 rpm, a reaction temperature of 65 °C, and a catalyst amount of 15 wt%.

3. Transesterification over the Bead-type Dolomite Catalyst for Bio-diesel Synthesis

The pretreated oil, for which the free fatty acid content was significantly lowered by lowering the initial acid value of the Jatropha oil from 11.8 mgKOH/g to 0.4 mgKOH/g or less through esterification, was used as a raw material for the transesterification reaction. The transesterification of Jatropha oil was performed in a Carberry spinning catalyst basket reactor equipped with a bead-type dolomite catalyst. The reaction conditions are a methanol/oil mole ratio of 10, 1 wt% of catalyst based on oil, a reaction temperature of 65 °C, and a stirring rate of 150 rpm. Fig. 8 shows the results of analyzing the FAME content by taking samples at every hour after the start of the reaction. As the reaction progressed, the FAME content increased, and after two to three hours equilibrium was reached. Fig. 8 shows the effect of the addition of pseudoboehmite sol, an inorganic binder added used in the catalyst forming process, on the reaction activity. At the beginning of the reaction, the Dolomite-bead-PB-10 catalyst showed the best performance, and the reaction activity decreased as the amount of pseudoboehmite sol was increased. This trend can be attributed to the reduced surface area and pore volume of the catalyst as the inorganic binder content was increased. However, the Dolomite-bead-PB-10 catalyst did not maintain the bead shape during the reaction, which

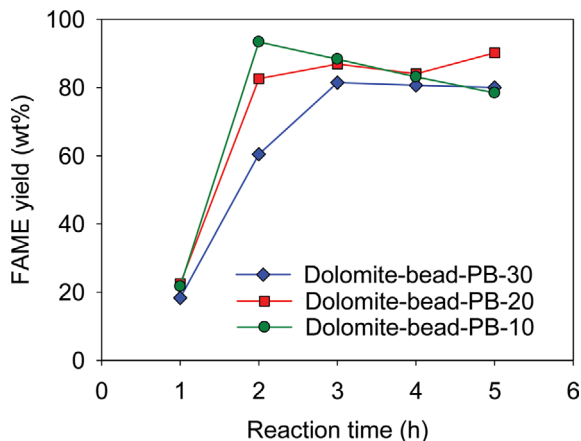


Fig. 8. Yield of FAME in transesterification over bead-type dolomite catalysts (reaction condition: methanol/oil mole ratio=10, reaction temperature=65 °C, stirring speed=150 rpm).

led to crumbling. Because the strength of the shaped catalyst is known to increase as the content of the inorganic binder increases [28,29], it can be confirmed that the surface area and strength of the catalyst exist in a compensatory relationship. As a result, it was found that the reuse of the Dolomite-bead-PB-10 catalyst was not feasible.

The Dolomite-bead-PB-20 catalyst showed more than 80% conversion after two hours of the reaction, showing superior activity compared to the Dolomite-bead-PB-30 catalyst. The Dolomite-bead-PB-20 catalyst and the Dolomite-bead-PB-30 catalyst were considered to be reusable because the shape and strength of the catalyst were maintained even after the reaction was completed. Consequently, among the bead-type dolomite catalysts prepared in this study, the Dolomite-bead-PB-20 catalyst was selected as the optimal catalyst for the transesterification reaction.

4. Regeneration of the Bead-type Dolomite Catalyst

After the transesterification reaction was completed, all of the

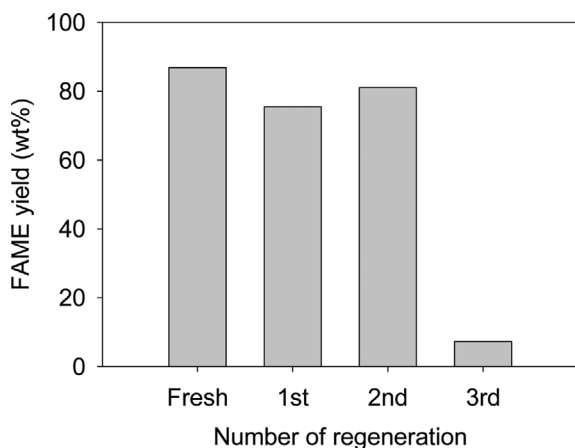


Fig. 9. Yield of FAME in transesterification over the fresh and regenerated Dolomite-bead-PB-20 catalysts (reaction condition: reaction time=2 h, methanol/oil mole ratio=10, reaction temperature=65 °C, stirring speed=150 rpm).

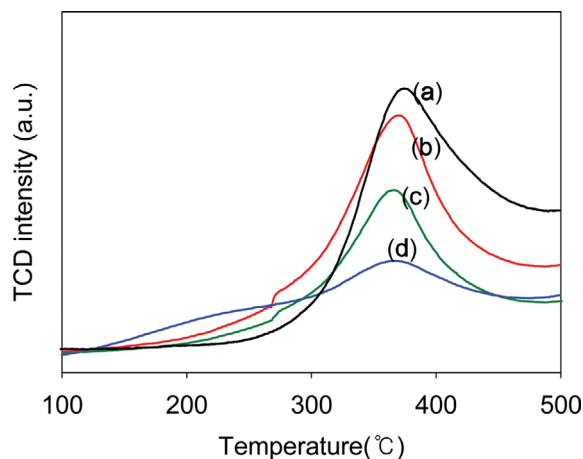


Fig. 10. CO₂-TPD results of the fresh and regenerated Dolomite-bead-PB-20 catalysts ((a) Fresh catalyst, (b) first regeneration, (c) second regeneration, (d) third regeneration).

products were recovered and the used Dolomite-bead-PB-20 catalyst was sequentially washed with methanol and dried in an air atmosphere as it was mounted in the catalyst basket. The regeneration method using methanol washing and drying was adapted because it is one of the regeneration processes with low-energy consumption. The regenerated catalyst was subjected to the transesterification reaction in a procedure identical to the reaction using the fresh catalyst. The results of transesterification using the regenerated catalysts are shown in Fig. 9. It was observed that the reaction activity of the catalyst when regenerated twice was recovered to a level similar to the reaction activity of the fresh catalyst, but the reaction activity was remarkably reduced in the catalyst when it was regenerated three times. That is, it was confirmed that the deactivated catalyst could not be regenerated after repeated use three times. As shown in Table 1, the BET surface area of the catalyst regenerated three times was reduced by nearly half compared to that of the fresh Dolomite-bead-PB-20 catalyst. The CO₂-TPD profile of the regenerated catalyst is compared in Fig. 10. Compared to the fresh catalyst, the number of basic sites of the catalyst regenerated once and twice did not significantly decrease. However, the number of basic sites of the catalyst regenerated three times was significantly reduced compared to that of the fresh catalyst. Therefore, it is likely that the reaction activity of the catalyst regenerated three times did not recover due to the loss of the basic sites of the catalyst surface.

Fig. 11 shows the results of an XRD analysis of the dolomite powder, the fresh Dolomite-bead-PB-20 catalyst, and the regenerated Dolomite-bead-PB-20 catalyst. It can be observed that peaks corresponding to CaO (JCPDS 00-037-1497) and MgO (JCPDS 01-078-0430) are dominant. CaO and MgO could be formed by the oxidation of CaMg(CO₃)₂ during the calcination procedure. In the fresh Dolomite-bead-PB-20 catalyst, CaO and MgO characteristic peaks are dominant, but Ca(OH)₂ (JCPDS 01-084-1263) and CaCO₃ (JCPDS 01-072-1937) characteristic peaks were also observed. For the catalyst regenerated once, a peak of Ca(C₃H₇O₃)₂ (JCPDS 00-021-1544) was also generated. It is known that

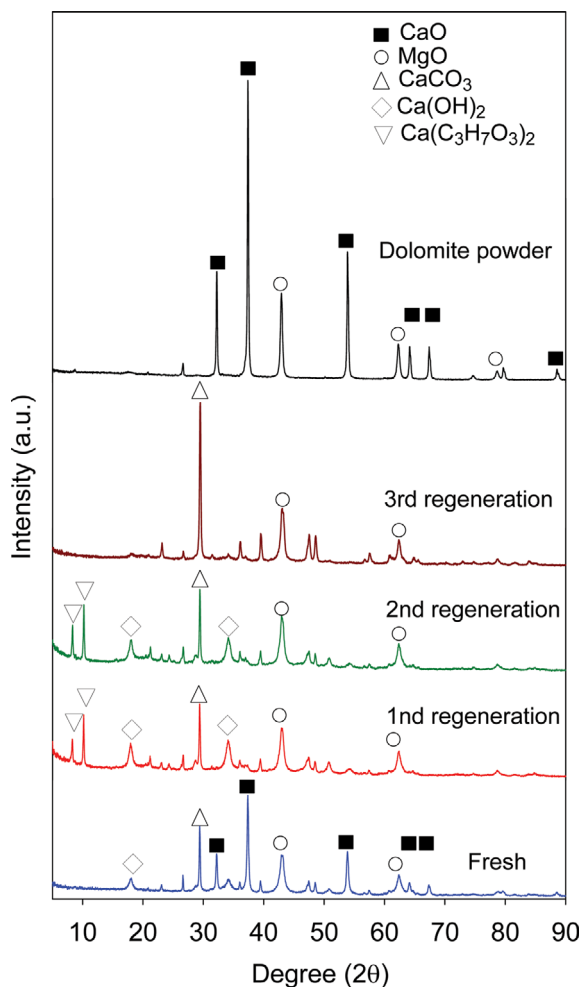


Fig. 11. XRD patterns of the dolomite powder and the fresh and regenerated Dolomite-bead-PB-20 catalysts.

$\text{Ca}(\text{C}_3\text{H}_7\text{O}_3)_2$ can be produced by the reaction of CaO and glycerin produced during the transesterification reaction [30]. In addition, it was confirmed that the height of the peak of CaCO_3 gradually became dominant with more instances of reuse. Also, in the catalyst regenerated three times, a small CaO peak and a $\text{Ca}(\text{C}_3\text{H}_7\text{O}_3)_2$ peak were observed, whereas the peak of CaCO_3 increased remarkably. Consequently, the Dolomite-bead-PB-20 catalyst nearly lost its active sites after three times of repeated regenerations, which can be attributed to the conversion of CaO to CaCO_3 during the regeneration and reuse procedure.

CONCLUSION

The acid value of Jatropha oil prepared in this study was 11.3 mgKOH/g, but it could be reduced to less than 0.4 mgKOH/g in 2 h of esterification using the Amberlyst-15 catalyst. Pretreated Jatropha oil was used as a raw material for transesterification in a Carberry spinning catalyst basket reactor equipped with a bead-type dolomite catalyst. Because the Dolomite-bead-PB-20 catalyst not only showed excellent activity in the transesterification reaction but also retained its strength and shape even after the reac-

tion was completed, it was selected as the optimal catalyst for the transesterification reaction. The used Dolomite-bead-PB-20 catalyst could be regenerated and reused twice without a loss of activity in transesterification. However, the regenerated catalyst nearly lost its active sites after three regeneration cycles, which can be attributed to the conversion of CaO to CaCO_3 during the regeneration procedure.

ACKNOWLEDGEMENTS

This research was supported by International Cooperation Program through the National Research Foundation of Korea (NRF-2019K1A3A9A01000010). This work was also supported by the Human Resources Program in Energy Technology of the Korea Institute of Energy Technology Evaluation and Planning (KETEP), granted financial resource from the Ministry of Trade, Industry & Energy, Republic of Korea (No. 20194010201730).

REFERENCES

1. A. C. Alba-Rubio, J. Santamaria-Gonzalez, J. M. Merida-Robles, R. Mareno-Tost, D. Martin-Alonso, A. Jimenez-Lopez and P. Maires-Torres, *Catal. Today*, **149**(3-4), 281 (2010).
2. Z. Yang and W. Xie, *Fuel Process. Technol.*, **88**(6), 631 (2007).
3. H. V. Lee, J. C. Juan and Y. H. Taufiq-Yap, *Renew. Energy*, **74**, 124 (2015).
4. A. Demirbas, *Energy Convers. Manag.*, **50**(7), 14 (2009).
5. A. P. Vyas, N. Subrahmanyam and P. A. Patel, *Fuel*, **88**(4), 625 (2009).
6. M. F. Rabiah Nizah, Y. H. Taufiq-Yap, U. Rashid, S. H. Teo, Z. A. Shajaratun Nur and A. Islam, *Energy Convers. Manag.*, **88**, 1257 (2014).
7. Y. Liu, H. Lu, W. Jiang, D. Li, S. Liu and B. Liang, *Chin. J. Chem. Eng.*, **20**(4), 740 (2012).
8. M. K. Lam, K. T. Lee and A. B. Mohamed, *Biotechnol. Adv.*, **28**(4), 500 (2010).
9. M. Agarwal, G. Chauhan, S. P. Chaurasia and K. Singh, *J. Taiwan Inst. Chem. Eng.*, **43**(1), 89 (2012).
10. L. Bournay, D. Casanave, B. Delfort, G. Hillion and J. A. Chodorge, *Catal. Today*, **106**(1-4), 190 (2005).
11. Y. H. Taufiq-Yap and N. Fitriyah, *Sains Malaysiana*, **40**(6), 587 (2011).
12. K. Colombo, L. Ender and A. A. C. Barros, *Egypt. J. Pet.*, **26**(2), 341 (2017).
13. M. Chai, Q. Tu, T. Lu and Y. J. Yang, *Fuel Process. Technol.*, **125**, 106 (2014).
14. O. Ilgen, *Fuel Process. Technol.*, **92**(3), 452 (2011).
15. M. O. Farque, S. A. Razzak and M. M. Hossain, *Catalysts*, **10**(9), 1 (2020).
16. I. M. Rizwanul Fattah, H. C. Ong, T. M. I. Mahlia, M. Mofijur, A. S. Silitonga, S. M. Ashrafur Rahman and A. Ahmad, *Front. Energy Res.*, **8**, 101 (2020).
17. H. Abdelsalam, H. H. EI-Maghrbi, F. Zahran and T. Zaki, *Korean J. Chem. Eng.*, **37**(4), 670 (2020).
18. P. Jasen and J. M. Marchetti, *IJLCT*, **7**(4), 325 (2012).
19. <https://www.chemengonline.com/catalyst-testing-design-selection-laboratory-reactors-2/?pagenum=1>.
20. M. Thommes, K. Kaneko, A. V. Neimark, J. P. Olivier, F. Rodriguez-

- Reinoso, J. Rouquerol and K. S. Sing, *Pure Appl. Chem.*, **87**, 1051 (2015).
21. S. Heo, M. Kim, J. Lee, Y. C. Park and J.-K. Jeon, *Korean J. Chem. Eng.*, **36**(5), 660 (2019).
22. N. J. A. Rahman, A. Ramli, K. Jumbri and Y. Uemura, *Sci. Rep.*, **9**(1), 1 (2019).
23. M. J. Kim, H. J. Kim, K.-E. Jeong, S.-Y. Jeong, Y. K. Park and J.-K. Jeon, *Korean J. Chem. Eng.*, **16**(4), 539 (2010).
24. D. Y. C. Leung, X. Wu and M. K. H. Leung, *Appl. Energy*, **87**(4), 1083 (2010).
25. J.-D. Choi, D.-K. Kim, J.-Y. Park, Y.-W. Rhee and J.-S. Lee, *Korean J. Chem. Eng.*, **46**(1), 194 (2008).
26. C. N. Satterfield, *Heterogeneous catalysis in industrial practice*, 2nd Ed., McGraw-Hill, New York, NY (1991).
27. J. Kim, J. Han, T. S. Kwon, Y.-K. Park and J.-K. Jeon, *Catal. Today*, **232**(1), 69 (2014).
28. F. Akhtar, L. Andersson, S. Ogunwumi, N. Hedin and L. Bergström, *J. Eur. Chem. Soc.*, **34**(7), 1643 (2014).
29. Z. Vajglova, N. Kumar, P. Maki-Arvela, K. Eranen, M. Peurla, L. Hupa and D. Y. Murzin, *Org. Process. Res. Dev.*, **23**(11), 2456 (2019).
30. M. Catarino, S. Martins, A. P. S. Dias, M. F. C. Pereira and J. Gomes, *J. Environ. Chem. Eng.*, **7**(3), 103099 (2019).